CrossMark

ORIGINAL ARTICLE

DFM method for aircraft structural parts using the AHP method

Charles Fortunet[1] · Séverine Durieux[1] · Hélène Chanal[1] · Emmanuel Duc[1]

Abstract During the part design process, the main objective is usually the maximum performance in use. For aircraft structural parts, the best ratio between mechanical resistance and weight is sought. However, these objectives can lead to geometries which are complex to manufacture. The DFM method presented here is based on concepts from morphological studies and analytic hierarchy process (AHP) to optimize the geometry of an I-Beam considering its manufacturing process and use. To do this, all the I-Beam alternatives that fit into the mechanical environment of the part are listed. Performance indicators are then defined to evaluate the weight, mechanical resistance, and manufacturability of each I-Beam. Then, performance indicators are compared and their relative priority measured on a ratio scale. Finally, the various I-Beam alternatives are compared using a macro-indicator composed of all the performance indicators in order to find the best geometry for the part considering its industrial and economic environment.

Keywords Design for manufacture · Machining processes · Morphological study · Analytical hierarchy process · Aircraft structural parts

✉ Charles Fortunet
   charles.fortunet@sigma-clermont.fr

   Séverine Durieux
   severine.durieux@sigma-clermont.fr

   Hélène Chanal
   helene.chanal@sigma-clermont.fr

   Emmanuel Duc
   emmanuel.duc@sigma-clermont.fr

[1] Université Clermont Auvergne, CNRS, SIGMA Clermont, Institut Pascal, 63000 CLERMONT-FERRAND, France

1 Introduction

Aircraft structural parts are designed in order to minimize the weight while ensuring the mechanical resistance requirements. Material and geometry are updated to obtain the best ratio between mechanical resistance and weight [1]. A lot of optimization algorithms have been developed in the literature to optimize the geometry of stiffened parts, but they do not take in to consideration the manufacturing of the computed geometry, usually [2, 3]. Herencia considers that design and manufacturing are uncorrelated and the manufacturing process must be adapted to the optimized geometry [4]. The problem can evolve if the economic aspect is taken into consideration. Indeed, the manufacturability does not affect the inflight performances of the part but the cost. To be competitive, designers have to take the manufacturing process features into account.

This paper presents a method dedicated to the optimization of structural part, taking into account mechanical and manufacturing requirements.

The application part is composed of a skin (exterior skin of the plane) and I-Beam stiffeners arranged in rectangular pockets (Fig. 1a). Two main steps are used for the manufacturing of the part: roughing by forging and finishing by milling. As forging is used for the roughing, minor geometrical variations can be permitted if the part located is the roughing volume of the part (Fig. 1b). During milling, the cost is directly linked to machining time. Particularly, the elongation, i.e., ratio between diameter (D) and length (L) (eq. (1)) of the tool impacts directly cutting conditions. Indeed, if the elongation increases, the stiffness of the tool will be reduced, so cutting conditions must also be reduced in the machining operation because vibration can appear due to the less in

⚛ Springer

Fig. 1 Part studied
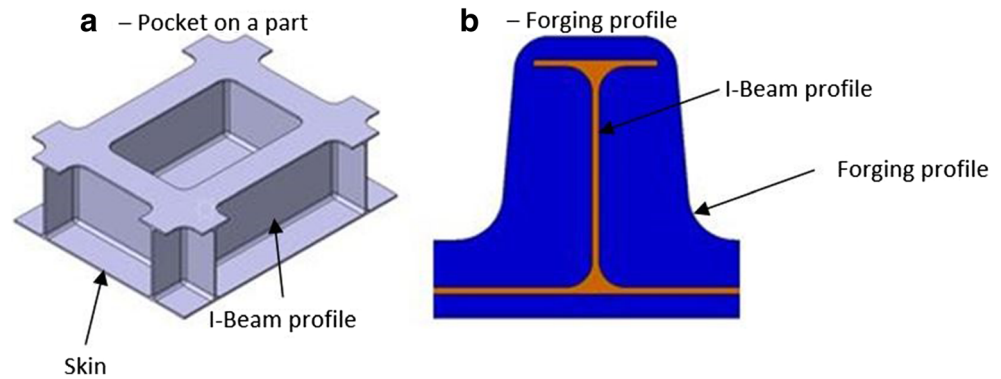
stability. As a consequence, the cost of the part increases. Usually, elongation's value is under 5. In this case, the elongation needed to machine the initial part in 16.

$$elongation = \frac{L}{D} \qquad (1)$$

In this paper, three objectives are defined for the optimization process: to minimize the weight, to keep the maximum mechanical resistance, and to reduce the manufacturing costs.

The proposed method is developed for a section of the application part: an I-Beam stiffener. Such feature is common in aircraft parts because the mechanical resistance is high for a low weight [5]. The disposition of the stiffeners in patterns reduces tool accessibility in 5-axis milling. Furthermore, vibrations can occur during the machining of the thin walls, and the generated surface roughness can thus be increased. According to the first experimental analysis, the area to be machined inside the I-Beam can be separated in two features: a lower feature machined in 5 axis with long tools and an upper feature machined with an angle head (AH).

As long as the geometry of the I-Beams is fixed, the process planning department has to find the best machining tool path while minimizing cutting efforts [6] and avoiding collisions [7–9].

For a complex part, a large amount of time is spent using particular strategies in order to reach a final geometry close to the CAD model. Features to be machined, requiring particular attention, are called masked entities [10] and are usually synonymous with a high increase of the machining time [11]. On the other hand, if the geometry can be modified, a discussion between design and process departments is necessary to define an acceptable variation of the part geometry that keep the inflight performances and increases the manufacturability of the part.

In this paper, the dimensions of an I-Beam profile are optimized taking into consideration the industrial and economic requirement of the part using analytic hierarchy process (AHP) method. The method is based on two concepts: a morphological box, which permits to evaluate a large set of solutions, and an AHP method to identify the best solution according to three different criteria, used in DFM.

First, a literature review is presented on the optimization methods. Then, the proposed method is described step by step and illustrated using the dedicated example. Finally, the extrapolation of the method to other types of profiles is discussed.

2 Literature review

In this part, concepts from design for manufacturing (DFM) and AHP are presented, and some examples are given.

2.1 Design for manufacturing

At the design stage, the designer must define the optimal geometry considering every stage of the lifecycle. Manufacturing requirements are usually not considered because they do not directly affect the performance of the aircraft in flight, but they affect the cost of the part at the beginning of the lifecycle. The DFM concept builds a link between design and manufacturing.

DFM methods for aeronautical parts can be implemented as expert system in CAD software to optimize a cost function made of a sum of manufacturing cost (expressed in $/m^2 of panel) and fuel burn cost (expressed in $/kg) to optimize the design of a fuselage panel [12]. On the other hand, Yin and Yu optimize the design of an aircraft wing highlighting the Pareto front that can be determined between the weight and the manufacturing cost [13].

DFM can be considered as a method to optimize the manufacturability of the design to tend toward a cost-effective manufacturing process [14] or a decision aid to define the most effective process. Kerbrat et al. provide a method that guides the designer to define a process based on machining and additive manufacturing [15]. In this case, the process is defined, and the geometry must be optimized to reduce manufacturing costs, depending on functional requirements. The importance of those requirements is not the same in the

decision-making process; thus, the weight is calculated with the AHP method. Ong proposes an AHP-based DFM method for designers to evaluate the manufacturability of designs. First, fuzzy set is used to generate *manufacturability indices* for each feature of the part. Then, AHP method is used to compare and weight features with respect to their functional importance. Finally, a manufacturability map is proposed for the designed part [16].

2.2 Analytic hierarchy process

The design of the studied part is complex, because every steps of the lifecycle must be taken into consideration. Thus, performance indicators are numerous. The literature proposes many multiple criteria decision-making methods and the applications are frequent in DFM. Usually, they are used to analyze and then optimize the manufacturability of designed parts, but none are developed for the pre-designing step [17].

The AHP method is able to aggregate a set of performance indicators in a macro-indicator that reflect the performance preferences of the decision maker in the associated industrial environment. The way to prioritize the indicators allows adapting the result more finely to the industrial environment that simplify discussion. Many AHP applications are implemented in industry [18]. For example, applications are found for scheduling to improve the productivity of a production line [19], for risk analysis to prevent supply chain crisis [20], or even as a basis for an algorithm made for resolving the multi-objective facility layout problems [21]. This method gives the opportunity to weight the indicators with a single decision maker or in a group decision-making environment [22].

AHP is a multi-criterion decision method that consists of sorting and grading a set of alternatives according to pre-established criteria [23]. In the first step, the decision maker compares criteria by pairs. Then, knowing the weight of each criterion, alternatives are compared by pairs to choose the best of the set. The coherence of the comparisons is controlled by a consistency ratio; however, the subjectivity of the judgment cannot be canceled [19]. Five steps are necessary to perform the method:

- *Step 1*: Decomposition of the problem into a hierarchical structure (containing three levels),
- *Step 2*: Binary comparison of the criteria in level 2 considering overall focus and calculation of their weight,
- *Step 3*: Measurement of the consistency of the judgment,
- *Step 4*: Binary comparison of the alternatives in level 3 considering each criterion in level 2 and calculation of their weight,
- *Step 5*: Calculation of the score of each alternative.

The DFM method developed in this paper uses concepts from AHP coupled with a morphological study; the next section focuses on the presentation of the method.

3 Presentation of the method

First, the method and the profile are presented. Next, a morphological study is used to determine the set of alternatives. Then, performance indicators are set up and prioritized using AHP. Finally, each alternative in the morphological box is compared to the others and the optimal alternative is highlighted.

3.1 General presentation

To optimize the geometry of an I-Beam, every possible alternatives for the profile are tested thanks to a morphological study [24], then the AHP is used to compare those profiles and highlight the optimal. Five steps are necessary to perform this optimization:

- *Step 1*: Parameterization of the profile
- *Step 2*: Construction of the morphological box
- *Step 3*: Creation and harmonization of the performance indicators
- *Step 4*: Prioritization of the indicators
- *Step 5*: Calculation of the macro-indicator

Usually, DFM methods using AHP are created to evaluate a part design [16] or to select the most effective process [25]. All these applications are applied to part that are already designed. The originality of this method concerns the coupling between DFM and AHP at the conceptual design stage. The aim is to give advices to the designer to optimize part profile. However, this method is influenced by the parameterization of the profile.

3.2 Parameterization of the profile

The method is developed for an I-Beam profile composed of three parts: two flanges (upper and lower) and a web. All the geometrical settings composing the beam are identified (H, l, e_v, e_h, r, r_{tra}) (Fig. 2). The output data of the algorithm is the set of optimized parameters corresponding to the optimal profile. A morphological box is used to define an exhaustive set of alternatives.

3.3 'Morphological box'

The parameter values are constrained by volumes filled by the equipments of the airplane. The designer fixes the limits for all the parameters, which must guarantee that any profile found
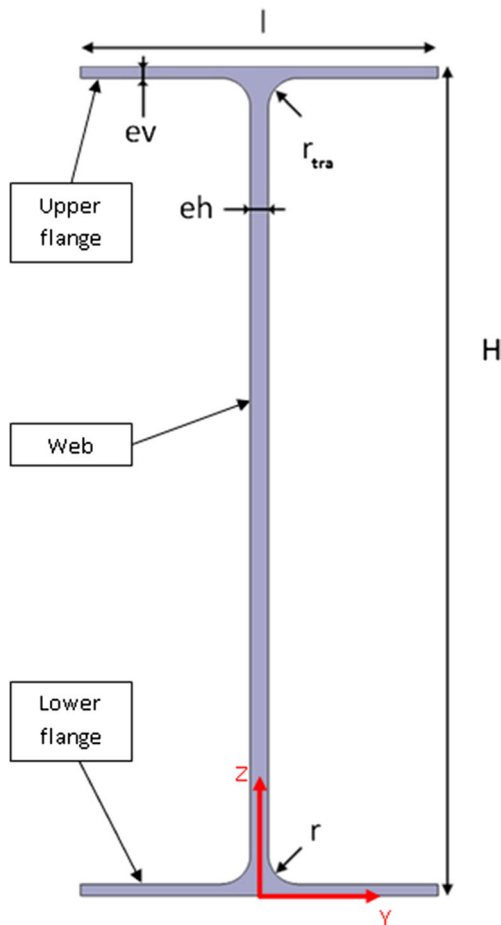
Fig. 2 Parameterization of the part

by the method is usable to the final shape of the part without major modifications. Then, values taken by each parameter at the end of the optimization are computed according to an increment step. The value of the step is determined by the expected accuracy of the results.

The morphological box is an N-dimensional matrix [S] (N is the number of parameters: 6 in our case). Thus, each cell of [S] contains a specific alternative geometry of the I-Beam profile. For example, the matrix [S] contains 48,125 alternatives (11 possibilities for H, 7 possibilities for l, and 5 possibilities for ev, eh, r, and r_{tra}), according to limits and steps of the morphological box. Every single alternative is rated using performance indicators reflecting the objectives of each stakeholder in the design process. The question is then to find the best alternative according to design and manufacturing considerations.

3.4 Creation and harmonization of the performance indicators

The performance objectives are expressed by numerical performance indicators to be compared in order to optimize the profile. The first step is to decompose the decision problem into a

hierarchical structure [26]. Here, the decision-making problem contains two levels: the first level contains indicators that express the stakeholder's objectives (weight, manufacturability, and mechanical resistance). From the manufacturability and mechanical resistance indicators, a second level of sub-indicators is defined to allow a finer transcription of the economical and industrial environment of the part. The weight indicator is accurate enough and does not need sub-indicators (Fig. 3).

In the following section, each indicator or sub-indicator is described and the calculation formulas are presented.

3.4.1 Mechanical resistance indicator

The mechanical resistance is the principal function of a structural part. During flight, the pressure difference between the inside and the outside of the aeroplane and the flight mechanics generate complex loading on the structure. The part must be designed to resist to this loading.

The real loading is too complex to be used for the optimization process. So, a simplified model is developed. Such model must be sufficiently accurate to discriminate profiles and easy to calculate. Loading can be simplified as compression in the upper part and tension in the lower part of the profile. Industrial experience shows that the mechanical behavior of the I-Beam is the sum of the behavior of two elementary surfaces reflecting compression or tension.

- *Elementary compression surface* (Fig. 4a): I-Beam profile with narrow lower flange equal to 30 times e_v.
- *Elementary tension surface* (Fig. 4b): I-Beam profile with large lower flange equal to the width of a pocket.

The mechanical resistance sub-indicators correspond to the quadratic moment (eq. (2)) of each elementary surface calculated at the center of gravity along the *Y*-axis.

- I_1: Quadratic moment of the *elementary tension surface*
- I_2: Quadratic moment of the *elementary compression surface*

$$for\ j \in [1, 2],\ \ I_j = \int_s x^2\ ds = \iint_s x^2\ dxdy \tag{2}$$

Maximum mechanical resistance is a requirement so these sub-indicators must be maximized. The mechanical resistance indicator (I) is a weighted sum of these sub-indicators (eq. (3)).

$$I = Coeff_{I1} \times I_1 + Coef\,f_{I2} \times I_2$$
With Coeff$_{I1}$ and Coef f$_{I2}$ the weight of the sub indicators I$_1$ and I$_2$
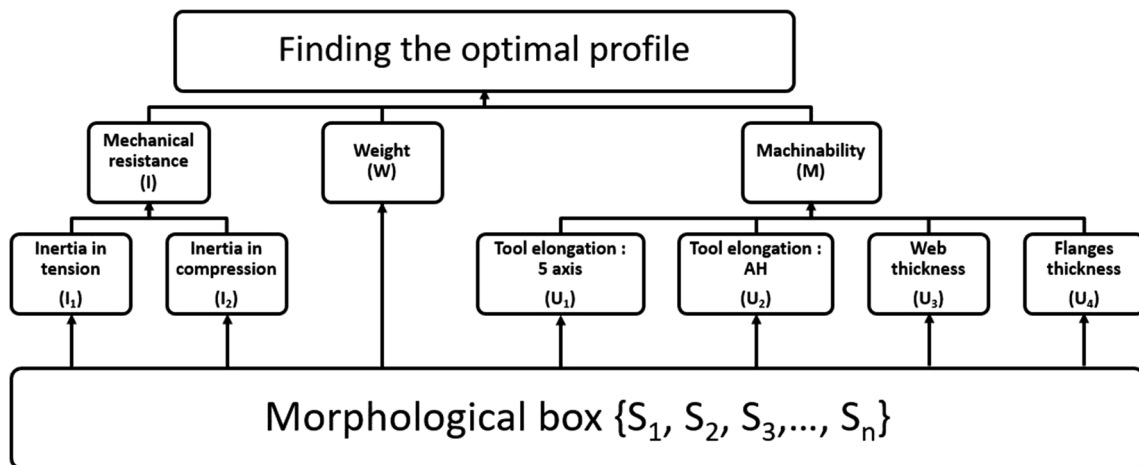
$$\tag{3}$$

Fig. 3 Hierarchical structure

3.4.2 Weight indicator

The material cannot be modified, so the weight of the part is directly linked to the area of the 2-dimensional profile. Equation (4) presents the formula applied to calculate the weight of the profile. The maximum performance is obtained by the lightest part so the weight indicator must be minimized.

$$W = 2(le_v) + (H-2e_v)e_h + 2\left(r^2\left(1-\frac{\pi}{4}\right)\right)$$
$$+ 2\left(r_{tra}^2\left(1-\frac{\pi}{4}\right)\right) \tag{4}$$

3.4.3 Machinability indicator

The machinability indicator is defined to ensure that the manufacturing cost is minimized during the optimization process. Two main considerations can be taken into account to evaluate the machinability of an I-Beam profile: the tool elongation and the wall thickness.

Tool elongation Tool elongation is the ratio between the tool's length and the diameter. Cutting conditions must be

Fig. 4 Elementary surfaces

chosen to avoid vibrations [27]: the longer the tool is, the less the stability is. The part must be designed to ensure that the machining process will be achievable without generating uncontrolled vibrations in the tool. The tool elongation (U_1) is calculated by a ratio between the shortest length L (Eq. (5)) and the maximum diameter ($2 \times r$) necessary to reach every surfaces to be machined. The security length L_1 is disregarded (Fig. 5a).

$$L = \sqrt{c^2-r^2} + r \quad with \begin{cases} a = \sqrt{\left(\frac{l-e_h}{2}\right)^2 + (h-2e_v)^2} \\ b = r\sqrt{2} \\ \beta = 45-\alpha = 45-atan\left(\frac{l-e_h}{2(H-2e_v)}\right) \\ c = \sqrt{a^2 + b^2 - 2abcos(\beta)} \end{cases}$$
$$\tag{5}$$

The radius r_{tra} cannot be reached with conventional 5-axis machining. A 90° angle head, equipped by a ball end cutter, is necessary. Previously, an elongation sub-indicator for the tool in the angle head (U_2) is calculated by the ratio between the minimum tool length necessary and the maximum diameter ($2 \times r_{tra}$). L_2 is disregarded in view of the other lengths (Fig. 5b). Equations (6) and (7) present the formula of the sub-indicators. To prevent vibrations, tool elongation must be minimized, i.e., U_1 and U_2 must be minimized.

$$U_1 = \frac{L}{2r} \tag{6}$$
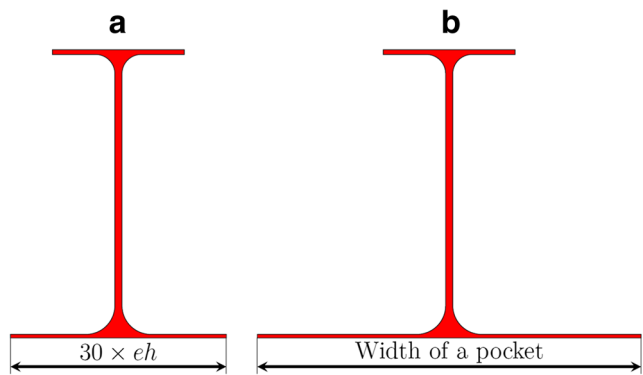
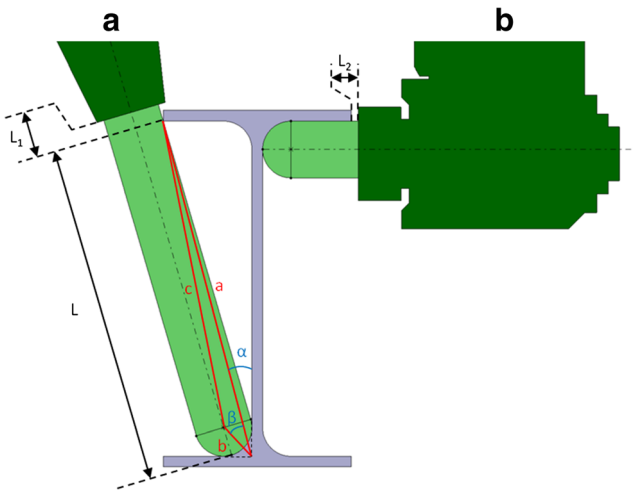$$U_2 = \frac{1-\frac{e_h}{2}}{2r_{tra}} \tag{7}$$

Fig. 5 Worst cases of tool location

Thin wall thickness The profile is composed of thin walls: the web and the flanges. The thickness of these walls must be controlled to minimize risks of bending or vibration during the machining process. A sub-indicator is defined for each thin wall (Eqs. (8) and (9)). To get the most stable process, the thickness of the walls (U_3 and U_4) must be maximized.

$$U_3 = \frac{e_h}{H-2e_v} \tag{8}$$

$$U_4 = \frac{2e_v}{l-e_h} \tag{9}$$

Machinability sub-indicators reflect risks during the machining operation. A minimal threshold value is set, to eliminate non-functional machining operations of the optimization process. Then, the machinability indicator (U) is calculated from a weighted sum of U_3 and U_4 with derived sub-indicators U_1' and U_2' calculated from U_1 and U_2 but to be maximized.

3.4.4 Control of the maximum variations of the indicators

The initial part is designed to present the best ratio between mechanical resistance and weight. In this optimization method, the manufacturability of the part is taken into consideration. This new consideration may require a decrease of the weight or the mechanical resistance indicator. To ensure that every tested alternative fit to the requirements, a lower bound is set for the indicator, if the bound is exceeded, the alternative is no longer taken into consideration. The bound is calculated as a percentage of the indicators of the initial profile; it is fixed by the authors at 95%.

3.4.5 Harmonization of indicators

Transformation of indicators The macro-indicator's value is calculated by a weighted sum of all the indicators. To get a coherent weighted sum, every term must be maximized. However, indicators W, U_1, and U_2 must be minimized, so a data transformation is performed as shown in eq. (10); derived indicators (W′, U_1', and U_2') to be maximized are defined from W, U_1, and U_2.

$$i \in [1, \text{nb } alternatives], \quad X \in \{W; U_1; U_4\}, X_i' = \max(X_i) - X_i \tag{10}$$

Normalization of indicators All the indicators (A, I, and U) are compared and weighted to obtain the macro-indicator, from a normalization step of indicators. Each indicator is divided by the maximum value reached in the morphological box. At this point, indicators are created, harmonized, and normalized. The fourth step of the method consists of using AHP concepts to determine the weight of the macro-indicator.

3.5 Prioritization of the indicators

Indicators will be compared by pairs to be prioritized. Comparisons are made numerically: for each pair of indicators, the degree of preference of one indicator is informed compared to the other. Table 1 present a scale for the prioritization proposed by Saaty.

Equation (11) presents the matrix [C] built using the values issued of the comparisons. Each cell C_{ij} corresponds to the comparison of a pair of indicators {i, j}. C_{ii} is naturally equal to 1 because an indicator cannot be compared to itself.

$$[C] = \begin{pmatrix} C_1 \\ \vdots \\ C_n \end{pmatrix} \begin{pmatrix} (C_1 & \cdots & C_n) \\ 1 & \cdots & C_{1n} \\ \vdots & 1 & \vdots \\ 1/C_{1n} & \cdots & 1 \end{pmatrix} \tag{11}$$

The priority vector [P] is calculated from the matrix [C], which gives the weight of each indicator. This method intends to an industrial application: the computational resources must be as low as possible so the priority vector is estimated by a method developed by Triantaphyllou [29].

When the vector is calculated, the coherence of the comparisons must be validated. Indeed, if C_1 is preferred twice as often as C_2, and if C_2 is preferred twice as often as C_3, then C_1 must logically be preferred four times more than C_3. Various methods have been developed to estimate the consistency of the judgment [30, 31]; the authors choose to use the consistency ratio (CR) method developed by Saaty to maintain low computational resource requirements. It is considered that the comparisons are coherent if CR is strictly under 10%; otherwise, judgments must be revised.

Table 1 Scale for indicator prioritization [28]

The fundamental scale for pairwise comparisons		
Intensity of importance	Definition	Explanation
1	Equal importance	Two elements contribute equally to the objective
3	Moderate importance	Experience and judgment moderately favor one element over another
5	Strong importance	Experience and judgment strongly favor one element over another
7	Very strong importance	One element is favored very strongly over another: its dominance is demonstrated in practice
9	Extreme importance	The evidence favoring one element over another is of the highest possible order of affirmation
Intensities of 2, 4, 6, and 8 can be used to express intermediate values. Intensities of 1.1, 1.2, and 1.3, etc. can be used for elements that are very close in importance		

To illustrate the adaptability of this method to the industrial environment, the authors decide to prioritize the indicators for two industrial cases.

3.5.1 Prioritization of indicators

- Case 1: Strong economic requirements: In this case, the economic requirement is predominant; to be competitive, the company must produce the part at the lowest cost. Machinability plays a strong importance compared to weight and mechanical resistance, which are of equal importance (Table 2a).
- Case 2: Strong environmental requirements: In the second case, the goal is to use the lowest possible fuel consumption according to ecological requirements. So, the plane must be as light as possible. However, the economic environment is also important to remain competitive, so the cost must also be controlled. In this case, weight has a strong effect on mechanical resistance and a moderate effect on machinability, so machinability plays a strong importance with respect to mechanical resistance

(Table 2b). For this application, a decrease of mechanical resistance is tolerated as long as the threshold for minimum mechanical resistance is not exceeded.

For both cases, priority vectors for the indicators ($[P_1]$ $[P_2]$) are calculated and the consistency of the judgment is verified.

3.5.2 Prioritization of sub-indicators

To simplify the example and the result analysis, only one case is studied for the sub-indicators. Authors choose to assign a great importance to the machinability sub-indicators U_1 and U_3 (tool elongation in 5-axis milling and web elongation) compared to U_2 and U_4 (tool elongation in the angle head and flange elongation). The decision maker considers that these are the most sensitive indicators in order to minimize the machining time (and thus the cost of the part). On the other hand, both of the mechanical resistance sub-indicators present the same importance (Table 3). Then, priority vector for

Table 2 Prioritization of the indicators

	Area	Inertia	Machinability		Area	Inertia	Machinability	Sum	$[P_1]$	CR
(a)										
Area	1.0	1.0	0.3	Area	0.20	0.20	0.19	0.59	*0.20*	*0.00%*
Inertia	1.0	1.0	0.3	Inertia	0.20	0.20	0.19	0.59	*0.20*	
Machinability	3.0	3.0	1.0	Machinability	0.60	0.60	0.63	1.83	*0.61*	
Sum	*5.0*	*5.0*	*1.6*							
(b)										
	Area	Inertia	Machinability		Area	Inertia	Machinability	Sum	$[P_2]$	CR
Area	1.0	5.0	3.0	Area	0.67	0.63	0.67	1.96	*0.65*	*0.32%*
Inertia	0.2	1.0	0.5	Inertia	0.13	0.13	0.11	0.37	*0.12*	
Machinability	0.3	2.0	1.0	Machinability	0.20	0.25	0.22	0.67	*0.22*	
Sum	*1.5*	*8.0*	*4.5*							

machinability [P_u] and mechanical resistance [P_{RM}] are calculated and the consistency of the judgment verified.

3.6 Calculation of the macro-indicator

The decision-making problem presented here contains two levels of indicators. One level of sub-indicators, used to calculate machinability and mechanical resistance indicators, and another level of indicators used to evaluate the performances of the part according to the objectives of each stakeholder. Dividing the problem into two levels of indicator allows a finer approach at the prioritization step of the method. AHP is applied separately to each level, and three priority vectors are generated (eq. (12)). The machinability and mechanical resistance indicators are calculated, respectively with U_1, U_2, U_3, U_4 and [P_u] and I_1, I_2 and [P_{MR}] (eq. (13)). Then, the macro-indicator, called score, is calculated (eq. (14)). The optimal profile presents the highest score.

$$[P_U] = \begin{bmatrix} Coef\,f_{U1} \\ Coef\,f_{U2} \\ Coef\,f_{U3} \\ Coef\,f_{U4} \end{bmatrix}, [P_{MR}] = \begin{bmatrix} Coef\,f_{I_1} \\ Coef\,f_{I_2} \end{bmatrix}, \quad (12)$$

$$[P] = \begin{bmatrix} Coef\,f_W \\ Coef\,f_I \\ Coef\,f_U \end{bmatrix}$$

$$U_i = \begin{bmatrix} U_{1_i} \\ U_{2_i} \\ U_{3_i} \\ U_{4_i} \end{bmatrix} \cdot [P_U] \quad and \quad I_i = \begin{bmatrix} I_{1_i} \\ I_{2_i} \end{bmatrix} \cdot [P_{MR}] \quad (13)$$

$$Score_i = \begin{bmatrix} W_i \\ I_i \\ U_i \end{bmatrix} \cdot [P] \quad (14)$$

3.7 Implementation of the method

The software used is developed with MatLab. Indeed, the matrix data management seems to be the easiest way to

conduct a morphological study with six variables. All the possible alternatives are recorded in a six dimensions' matrix. Each dimension contains every possible values of a parameter; thus, the final matrix contains every solutions of the problem. For each term in the matrix, the performance indicators of the related profile are calculated. Only the alternatives that respect the constraint of maximum variations outlined in Sect. 3.4.4 are kept for the optimization. Then, the performance indicators of the remaining alternatives are harmonized (Sect. 3.4.5) and their scores are calculated in a dedicated matrix.

The optimal profile (i.e., the profile that gets the best score) is selected and designed automatically by a specific link between MatLab and Catia software.

The initial profile is inserted in the software to calculate the maximum acceptable variation but also to determine numerically the benefit generated by the method. Indeed, the values of the performance indicators of the optimal profile are compared with the initial values in percentage.

4 Results

4.1 Numerical results

The optimal profiles depending on the case of study are presented on Table 4. For the case #1 (strong economic requirements), the optimal profile has shorter length (l) and bigger radiuses (r and r_{tra}). Those modifications allow a machining of the part with a lesser elongation to increase manufacturability (30%). On the other hand, a reduction is observed on the mechanical resistance (5%).

For the case #2 (strong environmental requirements), the same modifications on length and radiuses increase the machinability; the weight is optimized by reducing the thicknesses (e_h and e_v). To maintain the mechanical resistance, the global height (h) of the profile is increased. A degradation of less than 5% on mechanical resistance generates a gain of almost 10% in weight and 10% in machinability.
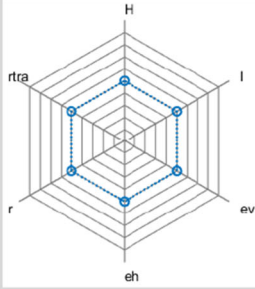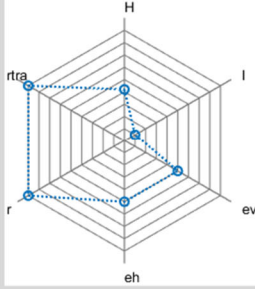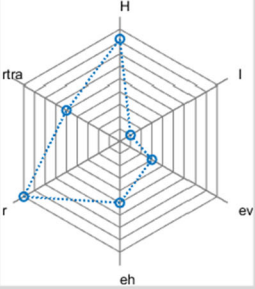
Both cases found by the method have different performances in accordance to the industrial environment modeled.

Table 3 Prioritization of the sub-indicators

	U_1	U_2	U_3	U_4		U_1	U_2	U_3	U_4	SUM	[P_u]	CR
U1	1.00	3.00	2.00	5.00	U_1	0.49	0.30	0.60	0.36	1.75	0.44	6.82%
U2	0.33	1.00	0.20	1.00	U_2	0.16	0.10	0.06	0.07	0.39	0.10	
U3	0.50	5.00	1.00	7.00	U_3	0.25	0.50	0.30	0.50	1.55	0.39	
U4	0.20	1.00	0.14	1.00	U_4	0.10	0.10	0.04	0.07	0.31	0.08	
Sum	2.0	10.0	3.3	14.0								
	l_1	l_2				l_1	l_2	Sum	[P_u]	CR		
l_1	1.00	1.00			l_1	0.50	0.50	1.0	0.50	0.0%		
l_2	1.00	1.00			l_2	0.50	0.50	1.0	0.50			
Sum	2.0	2.0										

Table 4 Comparison of optimization results with initial profile

Profile type	Initial profile	Case 1	Case 2
Design			
Mechanical resistance	0.0%	-4.37%	-3.27%
Weight	0.0%	-0.13%	-8.64%
Machinability	0.0%	+28.82%	+9.91%
Variables			

However, the length (l), the web thickness (eh), and the radius r have the same value in both cases. Only the height (H), the flange thickness (ev), and the radius r_{tra} impact the performances in the direction of case #1 and case #2.

4.2 Statistical analysis of the results

The maximum variation of the coefficient for the performance indicators sorts the alternatives in two categories: coherent or non-coherent, an alternative classified as non-coherent means that the machining is not possible or is not enough performing for an aeronautical process. On the 48,125 alternatives in the morphological box, only 533 are coherent. A statistical analysis is conducted to determine if the distribution of the alternatives is compact near the best alternative or if they are uniformly distributed on the entire domain of the score.

From Table 5, we can extract that:

- The distribution of the alternatives covers 11.7% (respectively, 15.8%) of the domain of the score ([0,1]) for case #1 (respectively, case #2).
- The second best score is 1.4% (respectively, 0.7%) lower than the optimal, which correspond to 6.9% (respectively, 1.5%) of the difference between the first and the last alternative.

- Mean and median are close and under the middle of the interval: 0.52 (respectively, 0.275). The density of alternatives is higher for lower values of the distribution.
- The initial profile is not optimized for those cases of study: #519 (respectively, #255) with a score of 0.475 (respectively, 0.259). The optimal profile generates a gain of 21.64% (respectively, 42.1%) compared to the initial profile.
- It appears that 0.72% (respectively, 1.99%) of the alternatives is on the 10% best scores and 33.45% (respectively, 23.69%) are on the better half of the distribution (Table 5).

This statistical analysis shows that this method generates a real gain on the performances of the initial profile and the optimal profile found is allowable compared to the other alternatives. However, to validate the relevance of the approach, it is necessary to verify if the comportment of the results is the same of a real aeronautical structural part.

4.3 Extrapolation to a real part

Based on the results of the morphological study, stiffened skins are designed to control the relevance of the performance

Table 5 Analysis of the macro-indicator's values

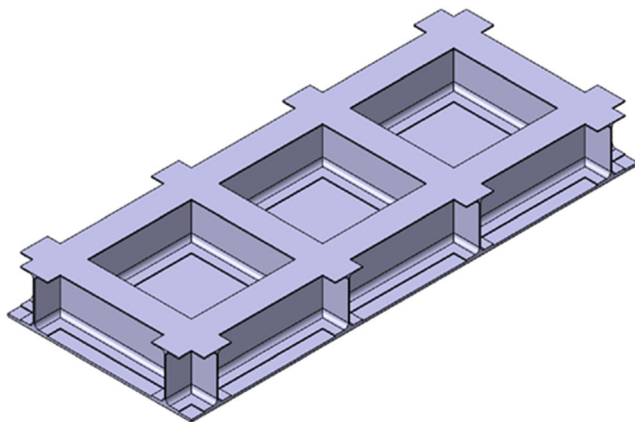|		Case 1	Case 2
Initial profile	Score	0.475	0.249
	Rank	#519	#255
profiles score	Profile #1 (best profile)	0.578	0.354
	Profile #2 (second profile)	0.570	0.352
	Profile #533 (worst profile)	0.462	0.196
Differences between profiles	#1 and #533 (absolute %)	11.7%	15.8%
	#1 and #2 (absolute %)	1.4%	0.7%
	#1 and #2 (relative %)	6.9%	1.5%
Analysis of the distribution	Mean score	0.510	0.253
	Median score	0.509	0.246
	Middle of the interval	0.520	0.275
	Alternatives with a score > 90% of the profile #1	4	11
		0.72%	1.99%
	Alternatives with a score > 50% of the profile #1	185	131
		33.45%	23.69%
Gain generated by the method		21.6%	42.1%

indicators. The profiles found are extruded and positioned in pockets and a skin is added (Fig. 6).

For each profile studied above, a part is designed. Then, their performances are calculated as follows:

- Weight: calculated on Catia V5 for a part in aluminum;
- Mechanical resistance: both extremities are fully fixed and a depression of 1 Bar is applied on the skin (Fig. 7a). The maximum displacement is calculated on Ansys (Fig. 7b);
- Machinability: the tool path to machine one pocket is programmed on Catia V5 and the machining time is calculated.

The results for those cases are described on Table 6:

Table 6 shows that the mechanical behavior for the entire parts follows the predictions of the indicators developed for

the method. The difference is reduced for the weight and the mechanical resistance. This reduction is due to the skin that is not taken into consideration in the method. For the machinability, the gain is higher than expected:

- On case 1, an increasing of 1.72% on the deformation allows a decreasing of 40% on the machining time while conserving the weight.
- On case 2, the increasing on the deformation is lower (1.38%) but allows a lighter part (3.12% less). In this case, the gain on machining time is lower (18.46% less long).

This study shows that the performance indicators are coherent with the mechanical behavior of an aeronautical structural part. Thus, we can consider that the profiles found with the morphological study match with the expectations.

Finally, we can consider that the model developed for this method represents the process design.

5 Discussions

The result and the analysis show that this method generates a significant gain on the performances of the I-Beam profile. Indeed, the prioritization and the morphological study allow tending toward the optimal profile taking into consideration the economical and industrial environment of the part. Constraints on the performance indicators insure that the chosen alternative fits to the aeronautical requirements. The statistical analysis of the results proves that the alternatives are not uniformly
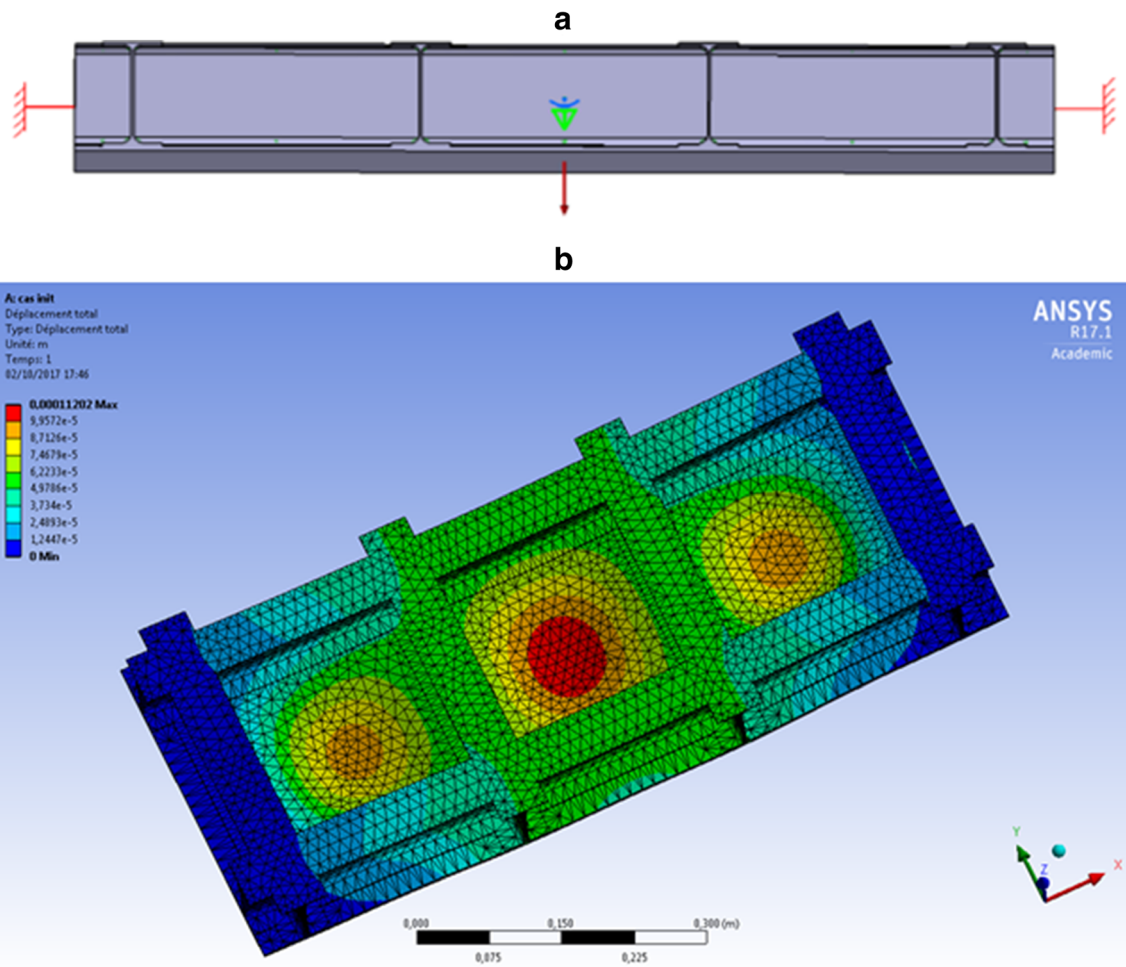

Fig. 6 Aeronautical structural part design based on the results

Fig. 7 Calculation of the performances of the aeronautical structural parts

distributed on the domain but a few fit most to the formulated requirements.

6 Conclusion

This paper presents a method to optimize the dimensions of an I-Beam profile to obtain optimal performances regarding the manufacturing stage of the life cycle. A morphological approach is used to generate a range of

Table 6 Performances of the aeronautical structural parts

	Initial case	Case 1	Case 2
Weight (kg)	6.929	6.967	6.713
	0%	0.55%	− 3.12%
Deformation (mm)	1.1202	1.1395	1.1357
	0%	1.72%	1.38%
Machinability (min)	25 min 33 s	14 min 31 s	20 min 50 s
	0%	− 43.18%	− 18.46%

alternatives to be tested. Next, performance indicators are set up and prioritized using AHP concepts to determine the weights in the decision process. Finally, the score of each alternative is computed from balanced sum of the indicators. The optimal alternative presents the best score at the end of the process. This optimization method is tested on two industrial cases with different constraints. In both cases, a benefit is observed using the optimal profile instead of the initial one. This optimization method could be improved by creating a link between optimized macro-geometries using the last stage of the AHP, which consists of comparing alternatives while considering each criterion. This method is a flexible tool, helping the designer in optimizing the part, taking into account the industrial and economic environment. An upgraded method will be considered, with the opportunity to compare various optimized macro-geometries and more complex parts.

References

1. Lutters E, Van Houten F, Bernard A, Mermoz E, Schutte C (2014) Tools and techniques for product design. CIRP Ann Manuf Technol 63:607–630. https://doi.org/10.1016/j.cirp.2014.05.010.

2. Mulani SB, Locatelli D, Kapania RK (2010) algorithm development for optimization of arbitrary geometry panels using curvilinear stiffeners. In 51st AIAA / ASME / ASCE / AHS / ASC structures, Structural Dynamics and Materials Conference doi:https://doi.org/10.2514/6.2010-2674.

3. Wang W, Guo S, Chang N, Yang W (2010) Optimum buckling design of composite stiffened panels using ant colony algorithm. Compos Struct 92:712–719. https://doi.org/10.1016/j.compstruct.2009.09.018

4. Herencia J, Enrique P, Weaver M, Friswell M (2008) Initial sizing optimisation of anisotropic composite panels with T-shaped stiffeners. Thin-Walled Struct 46:399–412. https://doi.org/10.1016/j.tws.2007.09.003

5. Mistry M, Gandhi F, Chandra R (2008) Twist control of an I-beam through Vlasov bimoment actuation. In 49th AIAA / ASME / ASCE / AHS / ASC Structures, Structural Dynamics and Materials Conference. doi: https://doi.org/10.2514/6.2008-2278.

6. Oda Y, Mori M, Ogawa K, Nishida S, Fujishima M, Kawamura T (2012) Study of optimal cutting condition for energy efficiency improvement in ball end milling with tool-workpiece inclination. CIRP Ann Manuf Technol 61:119–122. https://doi.org/10.1016/j.cirp.2012.03.034.

7. Wang N, Tang K (2007) Automatic generation of gouge-free and angular-velocity-compliant five-axis toolpath. CAD. Computer Aided Design 39:841–852. https://doi.org/10.1016/j.cad.2007.04.003.

8. Tang TD, Bohez E, Koomsap P (2007) The sweep plane algorithm for global collision detection with workpiece geometry update for five-axis NC machining. CAD. Computer Aided Design 39:1012–1024. https://doi.org/10.1016/j.cad.2007.06.004.

9. Tang TD (2014) Algorithms for collision detection and avoidance for five-axis NC machining: a state of the art review. Comput Aided Des 51:1–17. https://doi.org/10.1016/j.cad.2014.02.001.

10. Derigent W (2005) Méthodologie de passage d'un modèle CAO vers un modèle FAO pour des pièces aéronautiques : prototype logiciel dans le cadre du projet USIQUICK. PhD dissertation, Université Henri Poincaré, Nancy-I

11. Coelho RT, de Souza AF, Roger AR, Rigatti AMY, de Lima Ribeiro AA (2010) Mechanistic approach to predict real machining time for milling free-form geometries applying high feed rate. Int J Adv Manuf Technol 46:1103–1111. https://doi.org/10.1007/s00170-009-2183-8

12. Curran R, Gomis G, Castagne S, Butterfield J, Edgar T, Higgins C, McKeever C (2007) Integrated digital design for manufacture for reduced life cycle cost. Int J Prod Econ 109:27–40. https://doi.org/10.1016/j.ijpe.2006.11.010

13. Yin H, Yu X (2010) Integration of manufacturing cost into structural optimization of composite wings. Chin J Aeronaut 23:670–676. https://doi.org/10.1016/S1000-9361(09)60269-7

14. Andersson F, Hagqvist A, Sundin E, Björkman M (2014) Design for manufacturing of composite structures for commercial aircraft-the development of a DFM strategy at SAAB Aerostructures.

15. Procedia CIRP 17:362–367. https://doi.org/10.1016/j.procir.2014.02.053

15. Kerbrat O, Mognol P, Hascoët JY (2011) A new DFM approach to combine machining and additive manufacturing. Comput Ind 62:684–692. https://doi.org/10.1016/j.compind.2011.04.003

16. Ong SK, Sun MJ, Nee AYC (2003) A fuzzy set AHP-based DFM tool for rotational parts. J Mater Process Technol 138:223–230. https://doi.org/10.1016/S0924-0136(03)00076-1

17. Mardani A, Jusoh A, Zavadskas EK (2015) Fuzzy multiple criteria decision-making techniques and applications – two decades review from 1994 to 2014. Expert Syst Appl 42:4126–4148. https://doi.org/10.1016/j.eswa.2015.01.003

18. Vaidya OS, Kumar S (2006) Analytic hierarchy process: an overview of applications. Eur J Oper Res 169:1–29. https://doi.org/10.1016/j.ejor.2004.04.028.

19. Ohayon K, Ounnar F, Pujo P, Canal D (2011) Amélioration de l'ordonnancement d'une ligne de production par la méthode AHP. In 9e Congrès International de Génie Industriel CIGI.

20. Badea A, Prostean G, Goncalves G, Allaoui H (2014) Assessing risk factors in collaborative supply chain with the analytic hierarchy process (AHP). Procedia - Social Behavioral Sci 124:114–123. https://doi.org/10.1016/j.sbspro.2014.02.467

21. Singh SP, Singh VK (2011) Three-level AHP-based heuristic approach for a multi-objective facility layout problem. Int J Prod Res 49:1105–1125. https://doi.org/10.1080/00207540903536148

22. Altuzarra A, Moreno-Jiménez JM, Salvador M (2007) A bayesian priorization procedure for AHP-group decision making. Eur J Oper Res 182:367–382. https://doi.org/10.1016/j.ejor.2006.07.025

23. Saaty TL (1990) How to make a decision: the analytic hierarchy process. Eur J Oper Res 48:9–26. https://doi.org/10.1016/0377-2217(90)90057-I

24. Gogu G (2005) Evolutionary morphology. In: Bramley A, Brissaud D, Coutellier D, McMahon C (eds) Advances in integrated design and manufacturing in mechanical engineering. Springer, Dordrecht, pp 389–402. https://doi.org/10.1007/1-4020-3482-2_31

25. Desai S, Bidanda B, Lovell MR (2012) Material and process selection in product design using decision-making technique (AHP). European J Industrial Engineering 6:322–346. https://doi.org/10.1504/Ejie.2012.046666

26. Ounnar F, Khader S, Dubromelle Y, Prunaret JP, Pujo P (2013) Évaluation d'une méthode d'ordonnancement multicritère utilisant AHP. In 10° Congrès International de Génie Industriel CIGI.

27. Svoboda A, Tatar K, Norman P, Backstrom M (2006) Integrated approach for prediction of stability limits for machining with large volumes of material removal. Int J Prod Res 46:3207–3222. https://doi.org/10.1080/00207540601100924.

28. Saaty RW (1987) The analytic hierarchy process - what it is and how it is used. Mathematical Modelling 9:161–176. https://doi.org/10.1016/0270-0255(87)90473-8

29. Triantaphyllou E, Mann SH (1995) Using the analytic hierarchy process for decision making in engineering applications : some challenges. International journal of industrial engineering: theory, applications and. Practice 2:35–44

30. Saaty TL (1980) The analytic hierarchy process. McGraw-Hill, New York

31. Aguaron J, Moreno-Jiménez JM (2003) The geometric consistency index: approximated thresholds. Eur J Oper Res 147:137–145. https://doi.org/10.1016/S0377-2217(02)00255-2